DOI: 10.21062/mft.2023.089 © 2023 Manufacturing Technology. All rights reserved. http://www.journalmt.com

3D printing of Copper by Electrochemical Deposition Method

Michal Mišurák (0009-0008-3885-4868), Jan Šerák (0000-0003-3889-6618), Dalibor Vojtěch (0000-0002-6910-3206)
University of Chemistry and Technology Prague, Department of Metals and Corrosion Engineering, Technicka 5, 166 28 Prague 6 – Dejvice, Czech Republic. E-mail: serakj@vscht.cz

Additive manufacturing commonly also called 3D printing is a process which creates 3D structures according to digital 3D models by successive deposition of material layer by layer. Electrochemical 3D printing is a relatively new form of additive manufacturing, which creates metallic structures by electrochemical reduction of metallic ions from the electrolyte onto a conductive substrate. Advantages of this technology are ability to produce structures of several materials, without inert atmosphere, thermal stresses and without using laser optics. Theoretical part was focused on introduction to additive manufacturing and overview on its technologies, description of principle of electrochemical deposition, overview on electrochemical additive manufacturing technologies and influence of parameters, which affect it. Experiments were focused on effect of selected parameters of electrochemical 3D printing on print rate, mechanical properties, porosity, and microstructure of built structures of copper.

Keywords: Additive manufacturing, Electrochemical deposition, Copper, 3D print

1 Introduction

Additive manufacturing performs unique techniques which enable production of complex shaped parts by consecutive deposition of material layer by layer. Additively manufactured parts find their application in a lot of scientific fields including biomedical and aerospace industries. [1]. The most often used technologies for additive manufacturing of metallic materials are PBF (powder bed fusion) methods, which use laser or electron beam as an external source of energy for selective melting of metallic powders and their successive sintering according to a beforehand prepared model [2]. This way, sintered materials possess high residual stress due to a fusion at high temperature [3].

Electrochemical 3D printing offers a way to avoid this problem. Due to a non-thermal way of additive manufacturing, 3D printed structures have significantly lower residual stress. By electrochemical 3D printing, it is possible to print most of the conductive materials including metals, alloys, conductive polymers and even some semi-conductors [4].

Electrochemical 3D printing is based on the principle of electrochemical deposition of metallic ions from the electrolyte on to a conductive substrate. This deposition needs to be localized on a specified place [5].

The print head for localized electrochemical deposition is made from an electrode which is ended by a sharp tip and submerged into a bath of electrolyte containing ions of desired metal. Localized electrochemical deposition takes place when tip of the electrode which is connected as anode is very close to the substrate which is connected as a cathode. Electrical voltage is applied between these two electrodes. Consequently, reduction of metallic ions between cathode and anode and their deposition on the substrate exactly under the tip of anode takes place [6, 7].

The most important variable parameters that influence the process of localized electrochemical deposition are electrical voltage between cathode and anode, concentration of ions in the electrolyte, presence of several additives and materials which the tip and the substrate are made of. Optimal values of these parameters depend on the deposited material. Most of the studies that deals with the process parameters of localized electrochemical deposition are focused on metallic copper and nickel [8, 9]. Electric voltage has a significant influence on deposition rate and on porosity of 3D printed structures. The higher voltage is applied into the circuit, the higher current passes through it and therefore the deposition rate is higher. However, El-Giar et al. [8] measured the highest deposition rate at 4.3 V regardless of the highest current was measured at 4.8 V. The reason of this disharmony is local depletion of ions around of the tip at higher currents. When applied voltage exceeds a certain value, deposition current density may exceed limit current density, which can induce a formation of oxygen bubbles, which hinder the growth of the 3D printed structure and the deposition rate is then slowing. The printed structure shows porosity for that reason [8]. Therefore it is necessary to set the voltage and the print head movement velocity properly in order to get the highest

print rate with maintaining desired structural properties [10].

Kamaraj et al. [11] and Müller et al. [12] studied the influence of the distance between the tip of the anode and substrate on localized electrochemical deposition. According to them, a too small space between the tip and the substrate can cause inconsistent deposition due to local depletion of ions. On the other hand, the deposition is faster and more accurately localized at smaller spacings [11]. Kamaraj et al. [13] also printed a structure of nickel at extremely low spacing (5-10 μm). They have found out that at this small spacing, the deposition does not take place between the tip and the substrate due to the ion depletion. The deposition takes place only in the area near of the tip which results in the formation of hollow structure. Said et al. [10] focused on the print head movement velocity upwards in 3D printing of vertical structures. They simulated deposition profiles for three situations: movement of the print head slower, faster, and equal to the growth rate of the printed structure. In case of slower movement, an excessive deposition in lateral direction takes place, while the growth in the vertical direction is limited by the velocity of the movement of the print head. At extremely low velocity of the print head movement the deposition can even stop. If the movement of the print head is faster than the growth of the printed structure, a very porous structure is printed. At extremely fast movement the structure can be even hollow. At optimal conditions, when the velocity of the movement of the print head is equal to the growth of the printed structure, the most regular shape and most accurate dimensions can be achieved. Seol et al. [14] underlined the importance of mutual interplay between deposition ruled by diffusion and transport of charge and also suggested a new strategy for enhancement of lateral definition and lowering the porosity of 3D printed materials with RTG microradiography. Thanks to this technology, they have worked out the critical distance between the tip of the anode and the substrate, under which the deposition is ruled more by the charge transport which was the reason of formation of structures with higher porosity. Lin et al. [15] therefore suggested a process of intermittent localized electrochemical deposition, where in case of reduction of the distance between deposited structure and tip of the anode under a certain limit, the voltage drops to 0.5 V, the print head goes back until it touches the deposited structure and in that moment the print head shifts upwards to restore the beforehand set distance from the printed structure.

Yeo et al. [16, 17] dealt with mechanical ways to improve the properties of deposited structures and resolution of the 3D printing. Thanks to the rotating electrode, the deposition was more homogenous which led to reduction of the number of defects in the 3D printed structures. Thay have also suggested using ultrasonic vibrations which were continuously removing the oxygen bubbles formed during the deposition which were hindering the growth of the deposited structure. That way they enhanced the deposition rate and dimensional accuracy of the of the 3D printing process. Another way of oxygen bubbles removal was suggested by Lee et al. [18]. In their study they used horizontally oriented installation where the substrate was not lying on the building platform, but it was standing perpendicularly to it. The tip of the anode was approached to it from the side. Thanks to this orientation, the bubbles were running away upwards, and they did not get stuck under the tip of the anode.

Authors [19, 20] performed localized electrochemical deposition using pulsed voltage. According to them a pulsed voltage leads to higher current density and contributes to asymmetric distribution of current which induces formation of fine-grained structures with a smooth surface. They discovered that at higher voltage and longer working cycles, porous structures with a rough surface are formed. At lower voltage and shorter working cycles, denser structures with smoother surface were printed due to replenishment of the depleted ions under the tip between the working cycles.

Madden a Hunter [21] have printed a spring shaped nickel structure by localized electrochemical deposition which was hollow inside. At the voltage of 4.5 to 5 V they have achieved a print rate 360 μmmin^{-1}. The printed structure had an elasticity modulus of 200±120 GPa.

For localized electrochemical deposition of copper are most commonly used acidic sulphate baths [22]. Li et al. [23] observed the influence of concentration of H_2SO_4 on print rate on morphology of the printed structures deposited from the solution of $CuSO_4$. In case of using a bath with no H_2SO_4 asymmetric copper structures with a lot of branches were formed which were getting larger with increasing voltage. The deposition rate was high. After the addition of H_2SO_4, uniform non-branched structures with a constant diameter were formed at all voltages. However, the print rate was lower. The surface of the printed structures was smoother at higher voltage.

The 3D printing method using the principle of electrochemical precipitation of metals is promising for the preparation of very small porous samples. Most modern commercial 3D printing methods, on the other hand, are used to print objects (including porous ones) that are significantly larger [29-31]. The 3D printing method using the electrochemical principle is thus a highly specialized method for preparation of small porous conductive samples.

2 Materials and methods

2.1 Experimental device

A device for localized electrochemical deposition was assembled from a 3D printer Creality Ender 3 which was originally designed for FDM technology. Its shortest possible step is 0.1 mm in directions x, y and z. The printing space is 220 mm x 220 mm x 250 mm. Dimensional accuracy is 0.1 mm and layer thickness 0.1-0.4 mm. This 3D printer offers print head movement velocity 1-180 mms^{-1}. Thickness of the polymeric filament for this 3D printer is 1.75 mm. This 3D printer also offers a possibility of manual control of the print head.

The print head was composed from an insoluble anode made of platinum wire. The advantage of insoluble anode in contrast to the soluble is constant dimensions and no need to replace it. That makes to insoluble anode the only option for the print head for localized electrochemical deposition. The platinum wire of a diameter of 350 μm was inserted into the plastic cover made of PETG. The inner space was sealed with the acrylic resin VariDur 200 for a mechanical fixation of the wire and for more accurate localization of the deposition. After the sealing, the tip of the anode was mechanically ground on a grinding paper SiC with roughness P250 and polished on a diamond paste D2. The same grinding and polishing process was applied on a substrate as well.

The experimental device was assembled from the FDM 3D printer whose print head was replace with the insoluble platinum anode, Petri dish with the electrolyte of volume approx. 300 ml which was placed on the building platform of the 3D printer, the source of the direct voltage, amperemeter which was measuring the current flowing through the circuit and a voltmeter to measure the voltage between the anode and the substrate. On the bottom of Petri dish was a cathode created from a copper plate. The substrate was put on the cathode.

An attempt to print a 3D object according to a 3D model with the smallest possible print head movement velocity was performed on an assembled device. It was observed that the movement of the print head is too fast to print a layer of a required thickness. Therefore, a strategy of manual control of the print head movement by the wheel under the display was applied. The length of one step was chosen 0.1 mm because it was the shortest possible step. In every step the print head was kept at its position until the moment when a sudden increase of the current took place and the voltage dropped almost to zero indicating that the deposited structure touched the tip of the anode. At that moment, the print head was always moved up by 0.1 mm.

2.2 3D printing of copper

An electrolyte of concentration with 1M $CuSO_4.5H_2O$ and 1M H_2SO_4 was prepared for localized electrochemical deposition. The chemicals of the purity p. a. were used. Depositing reduction reaction took place on the cathode (1), while the oxidation reaction took place on the tip of the anode (2).

$$Cu^{2+} + 2e^- \rightarrow Cu \quad (1)$$

$$H_2O \rightarrow \frac{1}{2}O_2 + 2H^+ + 2e^- \quad (2)$$

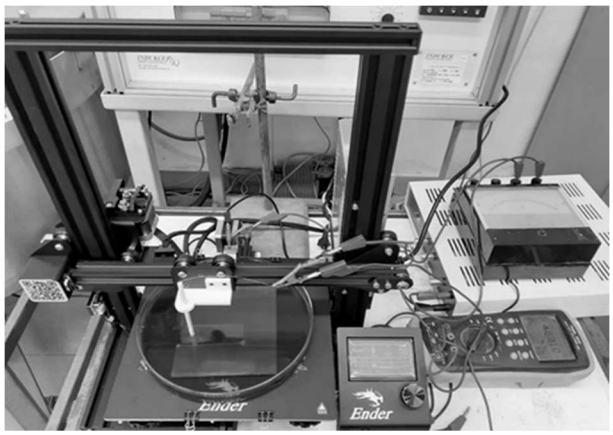

Fig. 1 *Experimental equipment for localized electrochemical deposition of copper*

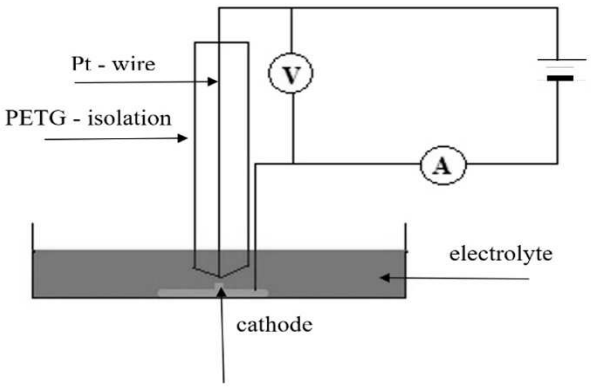

Fig. 2 *Scheme of the device for localized electrochemical deposition*

2.3 Numerical simulation of 2D current density distribution model

A numerical simulation of 2D model of current density distribution using the software COMSOL Multiphysics was performed with a Secondary Current Distribution method where electric resistance of electrolyte and kinetics of electrode reactions are considered. On the other hand, transport of the reactants is neglected considering the high concentration

of reactants on both electrodes. A conductivity of the electrolyte, anodic and cathodic potentiodynamic curves were measured using potentiostat Parstat 3000A-DX to acquire the input data. Three cathodic and three anodic curves were measured. The result values are determined by the average of the measurements.

2.4 Print rate determination

At first, experiments of printing a copper wire of the same diameter as that of the anode by moving the print head only in the z axis direction were performed. Several values of the voltage were applied to the circuit in these experiments. After every printed millimeter, the time from the beginning was recorded. A chart was created from the measured values. Eventually, an average velocity for each voltage was calculated as a slope of line determined by the measured points in the chart. Three measurements were performed for each voltage. The results were then statistically processed. A specimen of a cuboid shape of dimension 5 mm x 3 mm x 3 mm was printed at the chosen potential.

2.5 Preparation of metallographic samples

Metallographic samples were prepared from the chosen structures by submerging into acrylic resin VariDur 200 the way that they can be observed all along the side perpendicular to them print head movement direction. After the hardening of the resin, the samples were processed with a grinding paper of roughness P2500 and polished on diamond suspensions D2 and D0.7. Final polishing was done on colloid SiO_2 suspension Eposil F.

2.6 Observation of samples

As-printed samples and metallographic samples were observed by light microscope Nikon Eclipse MA200 with a digital camera TIS 5 MPix and software NIS Elements BR, stereomicroscope Olympus SZX10, and scanning electron microscope Tescan Vega 3 LMU.

2.7 Evaluation of porosity

Porosity was evaluated by a planar picture analysis using ImageJ software. Five pictures for each sample were evaluated. Results are the average values of all five analyses.

2.8 Measurement of hardness

Vickers hardness was measured using Future-Tech FM 700 machine on all metallographic samples. Measurements were done parallel plane to the print head movement direction with a load of 50 g and dwelling time of 10 s. Ten measurements were done on each sample and the result is the average of them all.

2.9 Uniaxial pressing test

Uniaxial pressing test using INSTRON 8802 machine was performed on a copper cuboid structure of dimensions of 5 mm x 3 mm x 3 mm. A stress necessary for the destruction of the structure was measured. The test was performed on the as-printed structure together with the substrate and on the copper plate of the same dimensions as the substrate afterwards.

3 Results and discussion

3.1 Print rate

Fig. 3 shows the chart of increase of length of 3D printed copper wires at several voltages. The experiments were done in a voltage range 3-5,5 V. The print rate at 3 V was so low that it was pointless to continue, and the experiment was stopped after 1 mm. At higher voltages, the wires were growing linearly with time. The print rate was constant. The highest print rate was recorded at voltage 5.5 V (1712 ± 81 μmmin^{-1}).

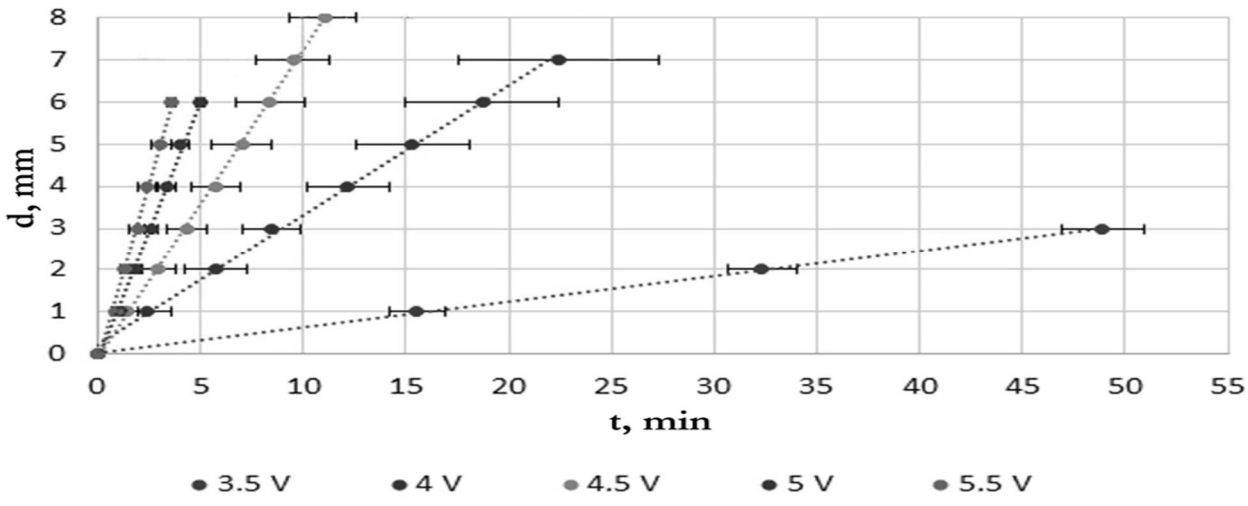

Fig. 3 *Print rates of 3D printed copper wires at different voltages*

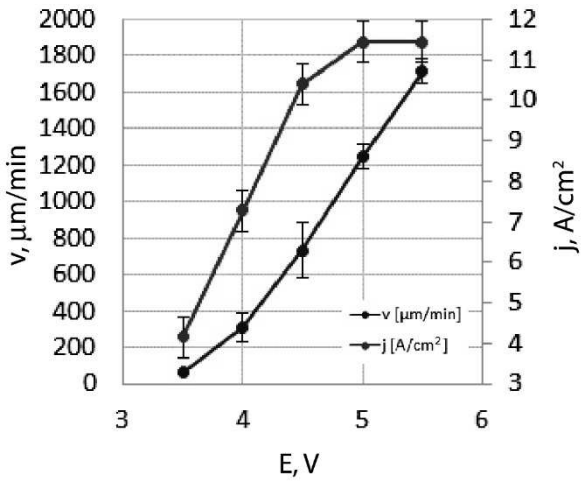

Fig. 4 *Dependence of print rate and current density on voltage*

There is a chart of print rate dependence on current density and voltage in the Fig.4. The chart displays directly proportional increase of print rate with current density. At voltage higher than 5 V no further increase of current density was observed, probably because of reaching limit current density. Experiments at higher voltages were not realized. The print rate was rising linearly with increasing voltage. The highest measured current density was 11.4 ± 0.5 Acm^{-2}. These values are approximately 2-3 orders of magnitude higher that those at conventional electrochemical deposition of copper [22]. Madden and Hunter [21], who performed localized electrochemical deposition of nickel also recorded 2 orders of magnitude higher current densities than in case of conventional electrochemical deposition. The highest print rate was 1712±81 μmin^{-1}. These values of print rate and current density are similar to ones measured by El-Giar et al. [8], who conducted similar experiments. However, they observed a decrease of current density and print rate above 4.5 V. This decrease was caused by a local depletion of ions in the area near of the tip of the anode.

3.2 Microstrucure

In Fig. 5a-d are images of 3D prints of copper deposited at voltages of 3.5 to 5 V. Diameter of copper wire deposited at 3.5 V (Fig. 5a) reaches values of 170-240 µm, which is approximately 1/2 to 2/3 of the platinum anode tip diameter. Microstructure of this wire is composed of rough dendrites which are interconnected and relates to each other, so they compose one compact unit with relatively smooth surface. Due to relatively low print head movement velocity 61±3 $\mu m min^{-1}$, dendrites were able to grow upward in the direction of 3D printing and connect to the other dendrites.

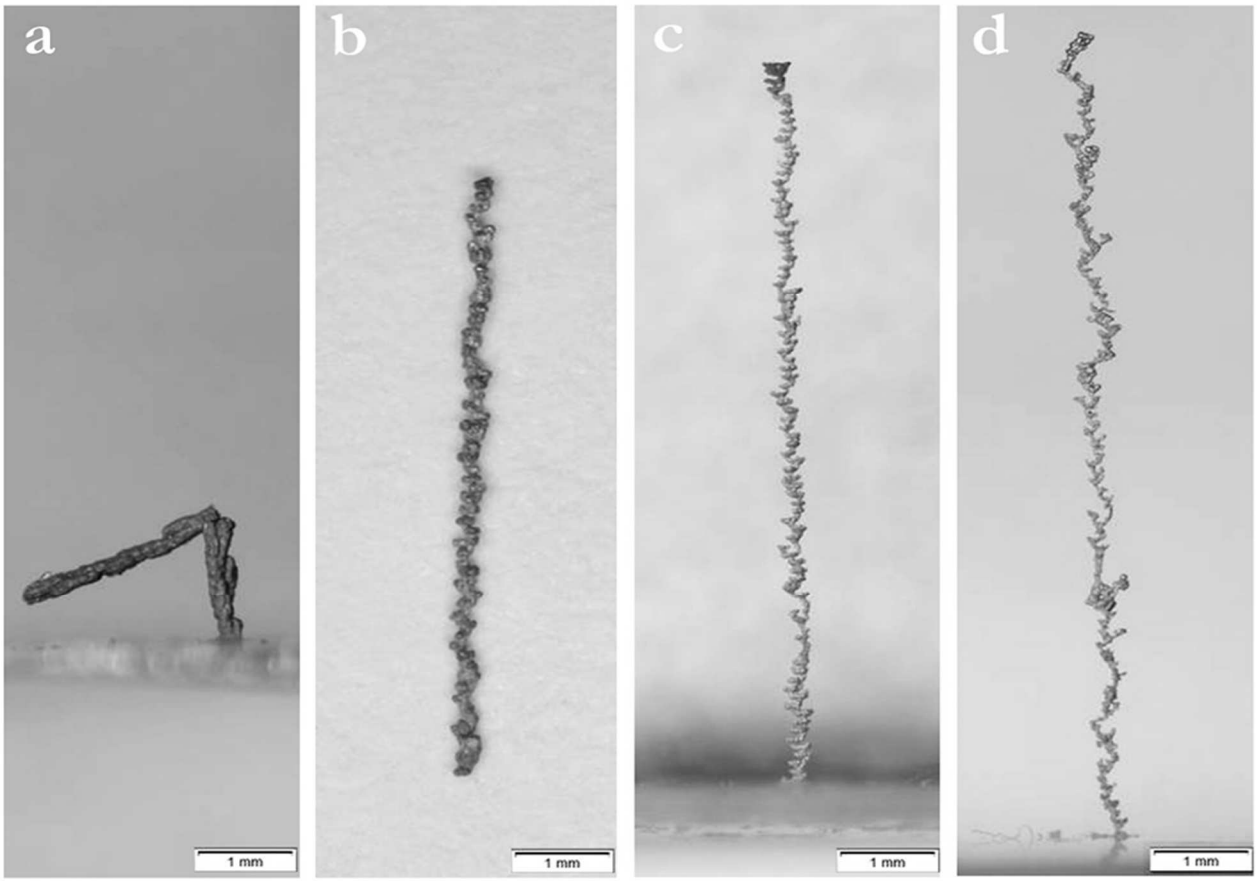

Fig. 5 *3D printed copper wires deposited at a) 3.5 V, b) 4V, c) 4.5 V and d) 5 V (stereomicroscope)*

Fig. 5b shows copper wire printed at 4 V. Print head movement velocity was at these conditions 309±91 μmmin^{-1} which is approximately 5 times higher than in previous case. Due to that, the forming dendrites were not able to connect with dendrites formed in the previous step which resulted in the formation of dissected surface with spacing between the dendrites of 31-40 μm. Diameter of the wire in the dendritic spots was 184-209 μm, thus a little lower than in case of 3.5 V.

Photographs of wire printed at voltage of 4.5 V are in the Fig. 5c. In this case, the print head was moving with the velocity of 732±172 μmmin^{-1}. The print rate was twice as high as at 4 V. The diameter in the dendritic spots was lowered to 157-178 μm. The microstructure was still dendritic, but a ladder-like shape can be observed which was caused by a step movement of the print head. Distance between the dendrites formed in steps increased to 43-53 μm.

In the Fig. 5d is wire created by 3D printing at voltage of 5 V. Print rate was 1247±78 μmin^{-1} at these conditions. That means that the print rate increased again to double the value reached at 0.5 V lower voltage. Diameter of the wire was reduced due to increased print rate again. In the locations with dendrites, the diameter reached values of 143-156 μm. These dendrites were thinner that in case of lower voltages. Their thickness is similar to the thickness in places with no dendrites in contrast to the dendrites created at lower voltages which are much thicker. Also, dendrites did not grow in each direction in plane perpendicular to the direction of print head movement, while at 4 and 4.5 V they did. The spacing between dendrites did not significantly change considering previous experiment and still reached values of 45-53 μm.

Figs. 5a-d show overview for comparison of 3D printed wires at selected voltages. Gradual reduction of diameter of printed structures both on the spots with and without dendrites can be observed. Decreasing dimensional accuracy of 3D printing with increasing voltage can be seen as well. Similar development of print rate and microstructure o printed structures was stated by Li et al. [23] and Chen et al. [24]. Another wire was printed at 5.5 V. 3D printing at this voltage confirmed trend of increasing print rate with increasing voltage (Figs. 3 and 4.). It also confirmed trend of reducing diameter with increasing voltage to such an extent that the 3D printed wire was broken during removal from the electrolyte. Manipulation with it was not possible due to very low mechanical properties. Its picture is missing for that reason.

For evaluation of the influence of the step size, another wire with step size of 0.2 mm was printed at 4.5 V. Its structure is shown in the Fig. 6. In comparison with the wire printed at the same voltage but with the step size of 0.1 (Fig. 5c), this wire was thicker, in the spots of dendrites it has 246-280 μm. The ladder-like structure can be observed also in this case, however distance between dendrites formed at consecutive steps was smaller than in case of printing with step size of 0.1 mm.

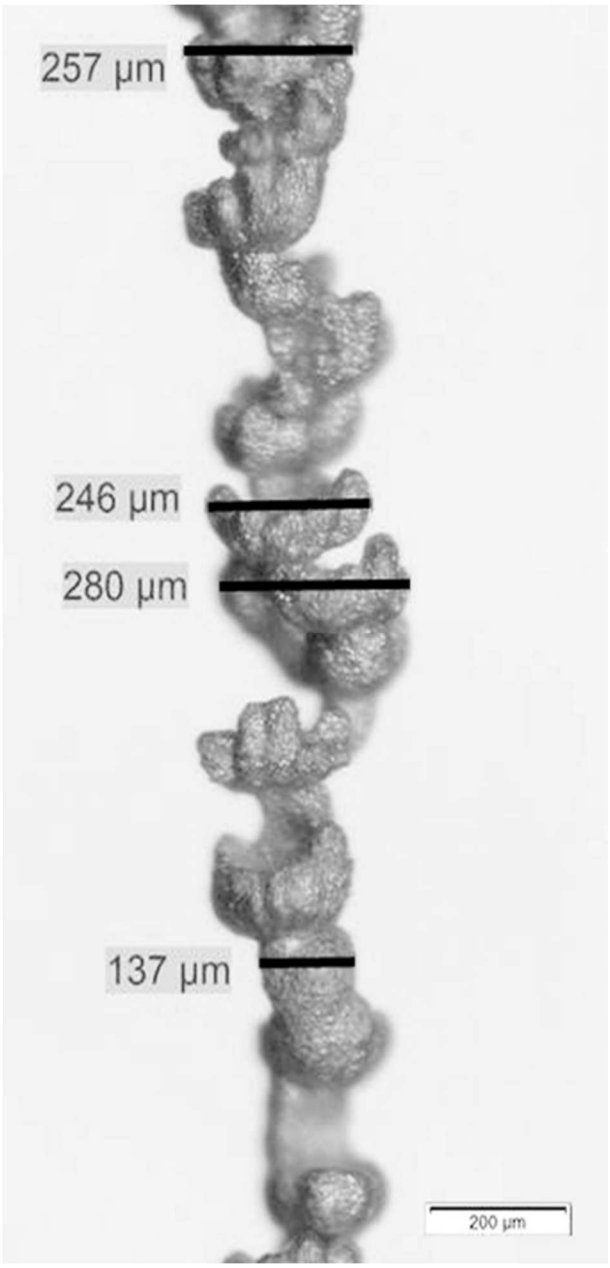

Fig. 6 *3D printed copper wire deposited at 4.5 V with the step size 0.2 mm (stereomicroscope)*

A disadvantage of conventional technologies of 3D printing of metals is a necessity of using supports when printing overhanging shapes [25]. Brant et al. [26] in their studies suggested that it was possible to print metallic structures with overhanging shapes without abutments by localized electrochemical deposition. For demonstration of this ability, a structure with perpendicular overhanging part was printed (Fig. 7).

ISSN 1213–2489
e-ISSN 2787–9402

Fig. 7 *3D printed copper structure with perpendicular overhanging part (stereomicroscope)*

3.3 Numerical simulation of 2D model of distribution of current density

For acquisition of input data for simulation a 2D model, cathodic and anodic potentiodynamic curves were measured. They are shown also with Tafel slopes in Fig. 12 and Fig. 13. Values of Tafel slopes, exchange current densities and equilibrium potentials for both cathodic and anodic curves are in the Tab. 1. These values were used as input data for numerical simulation. Other input data were the conductivity of the electrolyte 21.8 Sm^{-1}, distance between both electrodes 300 μm, voltage 5.5 V, limit current density $1.15.10^5$ Am^{-2} and diameter of the deposited structure 150 μm.

Tab. 1 *Tafel slopes, exchange current densities and equilibrium potentials for anodic and cathodic curves*

	Anodic curve	Cathodic curve
Tafel slope [V/decade]	0.08	0.15
Exchange current density [A/m²]	0.006	15.0
Equillibrium potential [V/SHE]	1.2	0.3

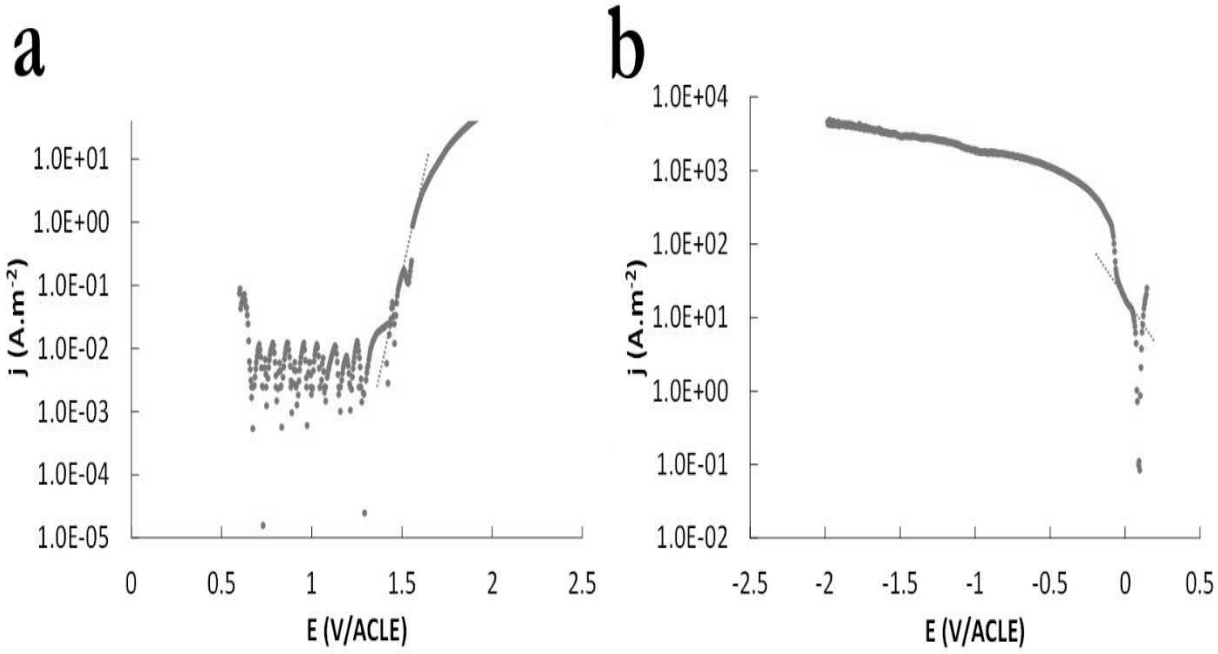

Fig. 8 *Potentiodynamic curves: a) anodic curve b) cathodic curve*

2D model of distribution of current density is in the Fig. 9. The localization of the current density in the area near of the tip of the anode is in the picture. This localization is even more intense during the 3D printing process after the nucleation of copper dendrites.

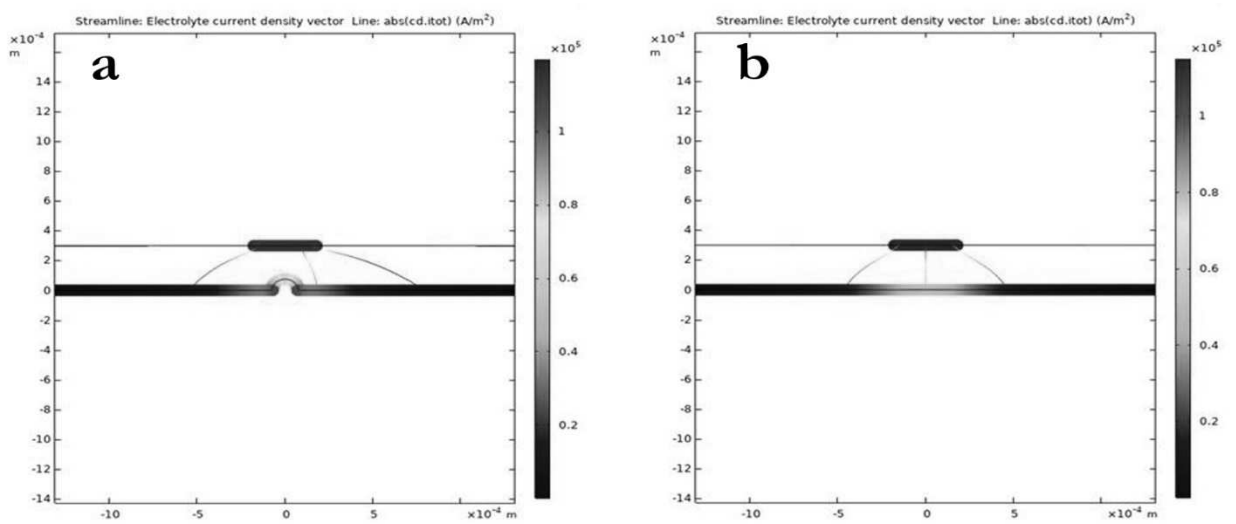

Fig. 9 *2D model of distribution of current density a) at the beginning of deposition, b) during 3D printing*

3.4 Porosity

The dependence of porosity of 3D printed samples on the selected voltages is shown in the Fig. 10. It can be observed that the porosity increases with increasing voltage and therefore with increasing print rate. The highest porosity was occurred at 5 V (59,6 ± 8,0 %). Similar relation between porosity and print rate was also confirmed by Chen et al. [27].

Fig. 11 shows pictures of metallographic samples of copper samples printed at different voltages.

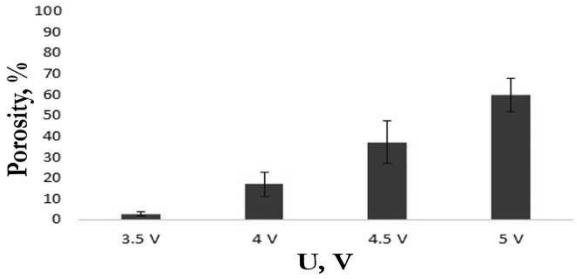

Fig. 10 *Porosity of 3D printed copper structures deposited at different voltages*

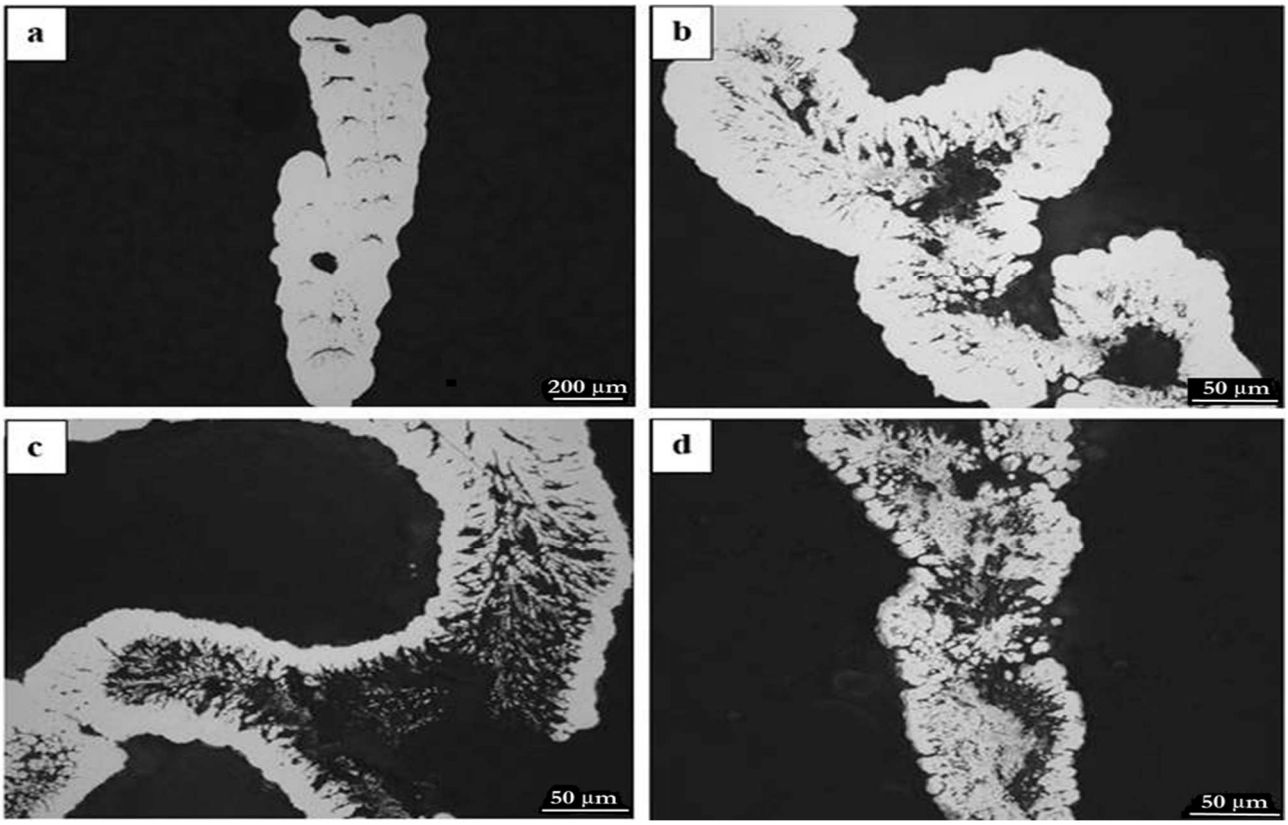

Fig. 11 *Metallographic samples of 3D printed copper wires deposited at a) 3.5 V, b) 4 V, c) 4.5 V, d) 5 V (light microscope)*

Porosity in prepared wires rises proportionally with increasing voltage and therefore with increasing print rate. In case of wire printed at 3.5 V, pores occurred only on the top of the dendrites. Their shape was semicircular, and they were curved around the dendrites. They were homogenously distributed throughout the whole sample. Fig. 11a also confirms that print rate at 3.5 V is slow enough for the dendrites to grow in the direction of the movement of the tip of the anode and interconnect with next dendrites. It can be seen in Fig. 11b and Fig. 11c that porosity increases at central parts of the wires at higher print rates. It is caused by unequal distribution of current. During electrodeposition of metals, electric current tends to concentrate at edges and ascended points [26]. For that reason, copper was deposited preferably at the edge of the wire in every step and successively filled the central part. This hypothesis is confirmed by the fact that the spot of occurrence of dendrites in created in each step always connects to the edge of copper dendrites formed in the previous step. Because of it, structures with helical shape were printed (Fig. 12).

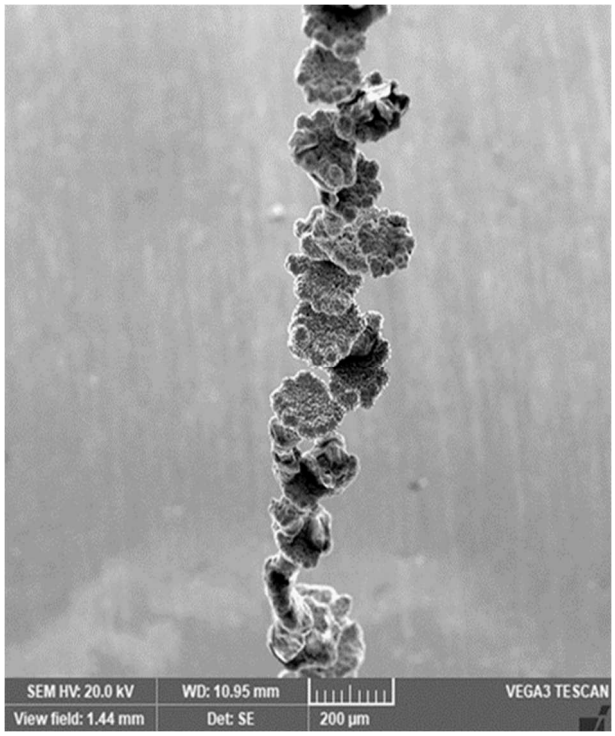

Fig. 12 *3D printed copper wire deposited at 4.5 V (SEM)*

The higher was the print rate, the less time it was for each step to be deposited. Therefore, the thickness of the pore less regions at the edge is reducing and the porosity in the central regions is increasing with increasing voltage. In case of wire printed at 4.5 V, central part is composed of very fine branched dendrites bounded by pores. Picture of this structure is in the Fig. 13. This picture confirms the increasing porosity in the direction into the central part of the sample.

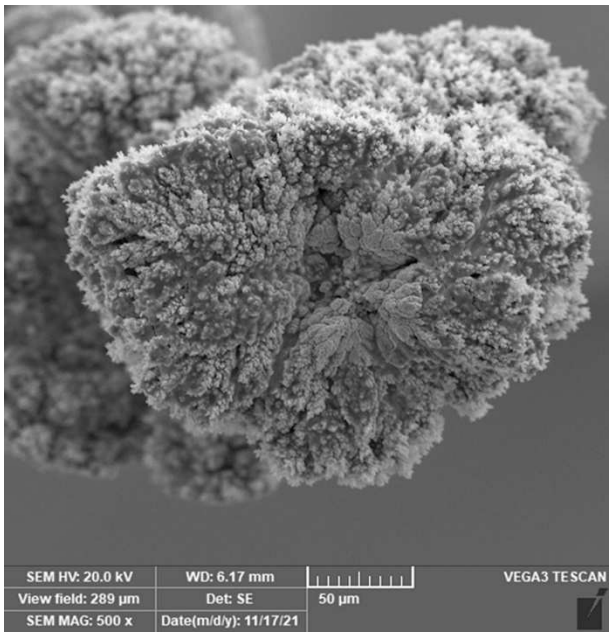

Fig. 13 *3D printed copper sample deposited at 4.5 V (SEM)*

3.5 Hardness

Measured values of porosity are confirmed by values of hardness (Fig. 14). Hardness of 3D printed copper samples decreases with increasing voltage, thus with increasing porosity.

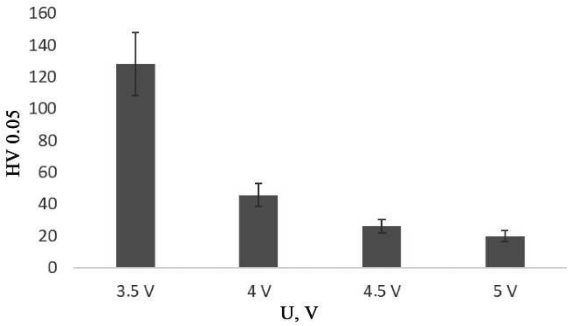

Fig. 14 *Hardness of 3D printed copper structures deposited at different voltages*

3.6 Uniaxial press test

Voltage of 4.5 V was chosen for 3D printing of cuboidal specimen with dimensions 5 mm x 3 mm x mm. This voltage was assumed to give an ideal compromise between print rate and mechanical properties. Strategy of hatching by one motion in parallel lines was applied for each layer. Trajectory of the movement of the print head was the same in each layer. Both layer thickness mm and hatch spacing were 0.3 mm.

Pictures of printed specimen are shown in the Figs. 15-17. The whole 3D printing process of this specimen took approximately 20 hours. Its porosity evaluated by picture analysis using ImageJ was 59±8 %.

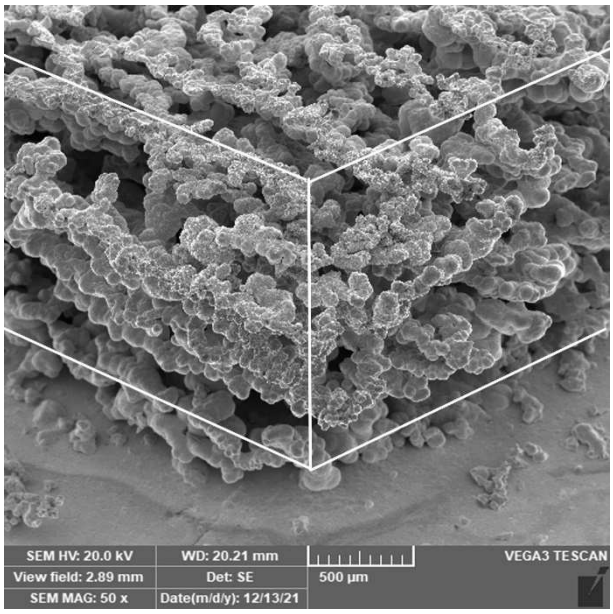

Fig. 15 *3D printed copper specimen of cuboidal shape deposited at 4.5 V (SEM)*

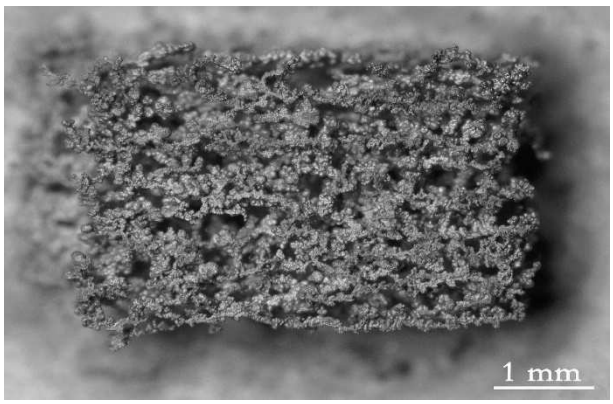

Fig. 16 *3D printed copper specimen of cuboidal shape deposited at 4.5 V on the copper sheet (stereomicroscope)*

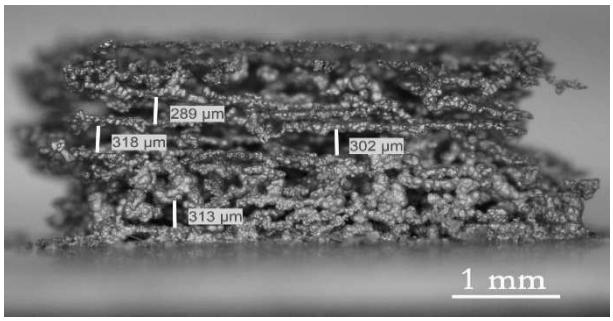

Fig. 17 *3D printed copper specimen of cuboidal shape deposited at 4.5 V (stereomicroscope)*

Uniaxial press test was performed on the 3D printed cuboidal specimen. From the perspective of area, pores were not considered. The chart of dependence of compressive stress on relative deformation of 3D printed specimen and the substrate alone is shown in the Fig. 18.

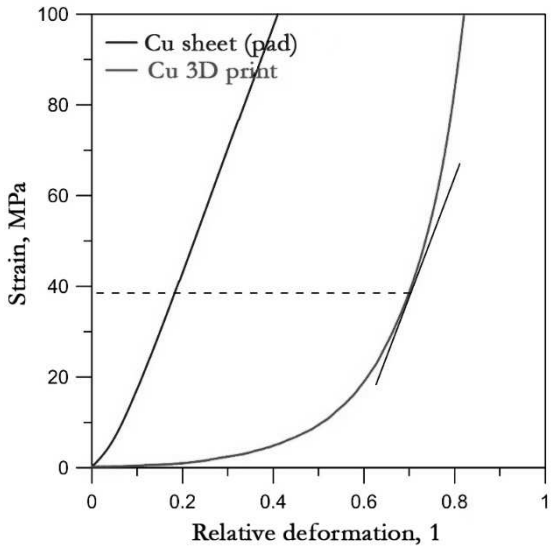

Fig. 18 *Stress-strain diagram for 3D printed specimen and substrate*

It can be observed that the curve for the substrate itself is steep and linear almost from the beginning, indicating elastic deformation. On the other hand, curve of the 3D printed specimen grows moderately and then it possesses convex shape (Fig. 19). A parallel line to the curve of the substrate tangential to the curve of 3D printed specimen was drown in the Fig. 18. The intersection of this parallel line and the curve of 3D printed specimen indicates the point of complete destruction of the specimen. After that, much bigger area than at the beginning was deformed because the deformation of the substrate takes place. For this reason, much bigger strength is needed for deformation and the compressive stress increases more rapidly. Thus, complete destruction of the specimen took place at the compressive stress 39 MPa.

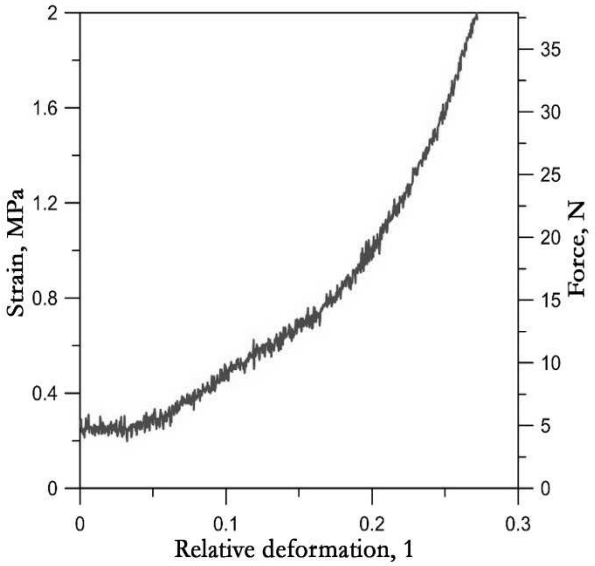

Fig. 19 *Detail of beginning of stress-strain curve for 3D printed specimen*

Fig. 19 shows detail of the beginning of the strain-stress curve for the 3D printed specimen. A spot where the curve changes from linear to convex is labeled by intermittent line. In this moment, elastic deformation probably turns into plastic. The specimen probably started to destruct at 0.75 MPa.

No cracking of the specimen was observed during the uniaxial press test. Deformation was continuous and the specimen was plastically destructed. The specimen after the test is shown in the Fig. 20.

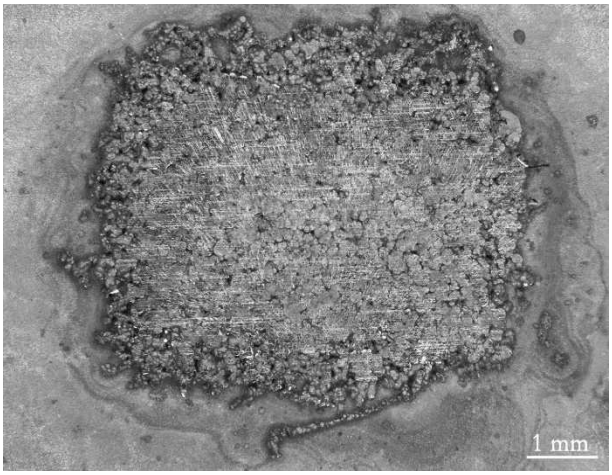

Fig. 20 *3D printed specimen after the uniaxial press test (stereomicroscope)*

4 Conclusion

In this study a 3D printer working on a principle of localized electrochemical deposition was designed. The printed material was copper which was reduced from the acidic bath of $CuSO_4$. Effect of voltage on print rate and microstructure of printed parts was evaluated by 3D printing of vertically oriented wires at different values of voltage. It was observed that print rate increases proportionally with increasing voltage. Consequently, dimensional accuracy thickness compactness and mechanical properties of the printed wires decreases, and porosity increases due to increasing print rate. Microstructure of the printed wires was dendritic at all voltages. These dendrites were getting finer with increasing voltage. In case of printing with bigger step, rougher microstructure was formed because of slower movement of the print head than it was in case of smaller step at the same voltage. Porosity of the printed material was increasing from the edge to the central part. Pores occurred mainly at the boundaries of the dendrites. Voltage of 4.5 V was selected for printing a cuboidal specimen. This specimen underwent an uniaxial press test. The specimen was plastically in the range of 0.75-39 MPa. Furthermore, another structure with perpendicular overhanging part which cannot be printed by conventional metallic 3D printing was successfully printed. At the voltage higher than 3.5 V ladder-like shaped structures were printed due to printed strategy step by step. The ideal solution of this problem might be a device which move the print head to maintain the constant distance between the tip of the anode and the printed structure. That way, continuous movement of the print head would be ensured and therefore more compact structures with smoother shape would be printed. In the further research, a 3D printer with stepping motor and higher resolution might be designed. Localized electrochemical deposition is a specific technology of metallic 3D printing and its application for 3D printing of microelectronic parts might be considered in the future.

Acknowledgement

Results of this work were obtained in the frame of the research project A1_FCHT_2023_009.

References

[1] GUO, N., LEU, M. C. (2013). Additive manufacturing: technology, applications and research needs. In: *Frontiers of Mechanical Engineering 2013*, Vol. 8, No. 3, pp. 215-243.

[2] YAP, C. Y., CHUA, C. K., DOG, Z. L., LIU, Z. H., ZHANG, D. Q., LOH, L. E., SING, S. L. (2015). Review of selective laser melting. In: *Materials and applications*. 2015, Vol. 2, No. 4, doi: 10.1063/1.4935926.

[3] KRUTH, J. P., LEVY, G., KLOCKE, F., CHILDS, T. H. C. (2007.) Consolidation phenomena in laser and powder-bed based layered manufacturing. In: *CIRP Annals 2007*, Vol. 56, No. 2, pp. 730-759.

[4] KADEKAR, V., FANG, W., LIOU, F. (2005). Deposition Technologies For Micromanufacturing: A Review. In: *Journal of Manufacturing Science and Engineering*, Vol. 126, No. 4, pp. 787-795.

[5] SUNDARAM, M. M., KAMARAJ, A. B., KUMAR, V. S. (2015). Engineering, Mask-less electrochemical additive manufacturing: a feasibility study. In: *Journal of Manufacturing Science*, Vol. 137, No. 2, doi: 10.1115/1.4029022.

[6] CHEN, X., BRANDON, N., CHILDS, P., WU, B., LIU, X. (2018). In: *Design and fabrication of a low cost desktop electrochemical 3D printer*, pp.395-400, doi: 10.25341/D4C01K.

[7] LIU, P., GUO, Y., WU, Y., CHEN, J., YANG, Y. (2020). A Low-Cost Electrochemical Metal 3D Printer Based on a Microfluidic System for Printing Mesoscale Objects. Vol.10, No. 4, doi: 10.3390/cryst10040257.

[8] EL GIAR, E., SAID, R., BRIDGES, G., THOMSON, D. (2000). Localized electrochemical deposition of copper microstructures. In: *Journal of the Electrochemical Society*, Vol. 147, No. 2, pp. 586-591.

[9] JASSON, A., THORELL, G., JOHANSSON, S. (2000). High resolution 3D microstructures made by localized electrodeposition of nickel. In: *Journal of the Electrochemical Society*, Vol. 147, No. 5, pp. 1810-1816.

[10] SAID, R. (2004). Localized electro-deposition (LED): the march toward process development. In: *Nanotechnology*, Vol. 15, No. 10, doi: 10.1088/0957-4484/15/10/025.

[11] KAMARAJ, A. B., SUNDARAM, M., (2018). A study on the effect of inter-electrode gap and pulse voltage on current density in electrochemical additive manufacturing. In: *Journal of Applied Electrochemistry,* Vol.48*,* No. 4, pp. 463-469.

[12] MÜLLER, A., MÜLLER, F., HIETSCHOLD, M. T. S. F. (2000). Localized electrochemical deposition of metals using micropipettes. In: *Thin Solid Films*, Vol. 366, No. 1-2, pp. 32-36.

[13] KAMARAJ, A. B., LEWIS, S., SUNDARAM, M. (2016). Numerical Study of Localized Electrochemical Deposition for Micro Electrochemical Additive Manufacturing. In: *Procedia CIRP*, No. 42, pp. 788-792.

[14] SEOL, S., K., PYUN, A., R., HWU, Y., Margaritondo, G., JE, J., H. (2005). Localized Electrochemical Deposition of Copper Monitored Using Real-Time X-ray Microradiography. In: *Advanced functional materials*. Vol. 15, No. 6, pp. 934-937.

[15] LIN, C. S., LEE, C. Y., YANG, J. H., HUANG, Y. S. (2005). Improved Copper Microcolumn Fabricated by Localized Electrochemical Deposition. In: *Electrochemical and Solid-State Letters,* Vol. 8, No. 9, pp. 125-129.

[16] YEO, S., CHOO, J. (2001). Effects of rotor electrode in the fabrication of high aspect ratio microstructures by localized electrochemical deposition. In: *Journal of micromechanics*, Vol. 11, No. 5, doi: 10.1088/0960-1317/11/5/301.

[17] YEO, S., CHOO, J., SIM, K. J. J. O. M. (2002). On the effects of ultrasonic vibrations on localized electrochemical deposition. In: *Journal of micromechanics*, Vol. 12, No. 3, doi: 10.1088/0960-1317/12/3/312.

[18] LEE, C., Y., LIN, C., S., LIN, B., R. (2008). Localized electrochemical deposition process improvement by using different anodes and deposition directions. In: *Journal of Micromechanics and Microengineering*, Vol. 18, No. 10, doi: 10.1088/0960-1317/18/10/105008.

[19] LIN, J., CHANG, T., YANG, J., CHEN, Y., CHUANG, C. (2010). Localized electrochemical deposition of micrometer copper columns by pulse plating. In: *Electrochimica Acta*, Vol. 55, No. 6, pp. 1888-1894.

[20] HABIB, M. A., GAN, S. W., RAHMAN, M. (2009). Fabrication of complex shape electrodes by localized electrochemical deposition. In: *Journal of Materials Processing Technology*, Vol. 209, No. 9, pp. 4453-4458.

[21] MADDEN, J. D., HUNTER, I. W. (1996). Three-dimensional microfabrication by localized electrochemical deposition. In: *Journal of Microelectromechanical Systems*, Vol. 5, No. 1, pp. 24-32.

[22] GIURLANI, W., ZANGARI, G., GAMBINOSSI, F., PASSAPONTI, M., SALVIETTI, E., DI BENEDETTO, F., CAPORALI, S., INNOCENTI, M. (2018). Electroplating for Decorative Applications. In: *Recent Trends in Research and Development*, Vol. 8, No. 8, doi: 10.3390/coatings8080260.

[23] LI, Y., LI, J., WANG, F. (2016). Localized electrochemical deposition of micrometer copper columns as affected by adding sulfuric acid. In: *Proceedings of 17th International Conference on Electronic Packaging Technology (ICEPT),* pp. 175-179.

[24] CHEN, X., LIU, X., CHILDS, P., BRANDON, N., WU, B. (2017). A low cost desktop electrochemical metal 3D printer. In: *Advanced Materials Technologies*, Vol. 2, No. 10, doi:10.1002/admt.201700148.

[25] HUSSEIN, A., HAO, L., YAN, C., EVERSON, R., YOUNG, P. (2013). Advanced lattice support structures for metal additive manufacturing. In: *Journal of Materials Processing Technology*, Vol. 213, No. 7, pp. 1019-1026.

[26] BRANT, A., SUNDARAM, M. (2016). A Novel Electrochemical Micro Additive Manufacturing Method of Overhanging Metal Parts without Reliance on Support Structures. In: *Procedia Manufacturing*, Vol. 5, pp. 928-943.

[27] CHEN, X., BRANDON, N., CHILDS, P., WU, B., LIU, X. (2018). Design and Fabrication of a Low Cost Desctop Electrochemical 3D Printer. In: *Proc. Of the 3rd*

Intl. Conf. on Progress in Additive Manufacturing (Pro-AM 2018), pp. 395-400, ISSN: 2424-8967.

[28] ŠERÁK, J., VOJTĚCH, D., NOVÁK, P., BÁRTOVÁ B. (2005). Preparation of nanosized copper powder by chemical leaching. In: *Proceedings of conference DF PM 2005,* Stará Lesná 27.-30. 09. 2005, Slovakia, pp.117-123, ISBN: 80-968543-4-8.

[29] CHALUPA, V., STANEK, M., VANEK, J., STRNAD, J., OVSIK, M. (2023). Design of Dual-Head 3D Printer. In: *Manufacturing Technology*. Vol. 23, No. 2, pp. 177-185. doi: 10.21062/mft.2023.032.

[30] JABBAR, M., A. (2023). A Design of Experiment Analysis Approach to Improve Part Quality in 3D Printing. In: *Manufacturing Technology*. Vol. 23, No. 3, pp. 290-297. doi: 10.21062/mft.2023.034.

[31] MATUŠ, M., BECHNÝ, V., JOCH, R., DRBÚL, M., HOLUBJÁK, J., CZÁN, A. (2023). Geometric Accuracy of Components Manufactured by SLS Technology Regarding the Orientation of the Model during 3D Printing. In: *Manufacturing Technology*. Vol. 23, No. 2, pp. 233-240. doi: 10.21062/mft.2023.027.